Development of a digital fluorescence sensing technique to monitor the response of macrophages to external hypoxia

Jacob K. Asiedu
Jin Ji
Mai Nguyen
University of New Orleans
Department of Chemistry
New Orleans, Louisiana 70148

Nitsa Rosenzweig
Xavier University of Louisiana
Department of Chemistry
New Orleans, Louisiana 70125

Zeev Rosenzweig
University of New Orleans
Department of Chemistry
New Orleans, Louisiana 70148

Abstract. Oxygen plays a very important role in living cells. The intracellular level of oxygen is under tight control, as even a small deviation from normal oxygen level affects major cellular metabolic processes and is likely to result in cellular damage or cell death. This paper describes the use of the oxygen sensitive fluorescent dye tris (1,10-phenanthroline) ruthenium chloride [$Ru(phen)_3$] as an intracellular oxygen probe. $Ru(phen)_3$ exhibits high photostability, a relatively high excitation coefficient at 450 nm (18 000 M^{-1} cm^{-1}), high emission quantum yield ($\sim$0.5), and a large Stoke shift (peak emission at 604 nm). It is effectively quenched by molecular oxygen due to its long excited state lifetime of around 1 μs. The luminescence of $Ru(phen)_3$ decreases with increasing oxygen concentrations and the oxygen levels are determined using the Stern–Volmer equation. In our studies, J774 Murine Macrophages are loaded with $Ru(phen)_3$, which passively permeates into the cells. Fluorescence spectroscopy and digital fluorescence imaging microscopy are used to observe the cells and monitor their response to changing oxygen levels. The luminescence intensity of the cells decreases when exposed to hypoxia and recovers once normal oxygen conditions are restored. The analytical properties of the probe and its application in monitoring the cellular response to hypoxia are described. © *2001 Society of Photo-Optical Instrumentation Engineers.* [DOI: 10.1117/1.1344190]

Keywords: fluorescence probes; oxygen; murine macrophages.

Paper CARD-02 received Oct. 1, 2000; accepted for publication Nov. 27, 2000.

1 Introduction

Oxygen is one of the key metabolites in aerobic systems. The rate of oxygen uptake is a good indicator of metabolic activity of cells. The oxygen concentration inside cells is of primary importance in determining numerous physiological and pathological processes in biological systems. Intracellular level of oxygen is under tight control, as even a small deviation from normal oxygen levels would cause major cellular damage or even cell death. The determination of oxygen in tumor cells for instance may lead to the treatment and prediction of the response of the tumor to therapy.[1] The level of intracellular analytes including molecular oxygen can be significantly altered when cells are exposed to hypoxia since the condition of hypoxia induces the production of intracellular reactive oxygen species (ROS).[2,3]

ROS are extremely reactive and display a short half life and low steady state concentration. Examples of ROS are superoxide radical (O^{2-}), hydrogen peroxide (H_2O_2), singlet oxygen ($^1O_2$), hydroxyl radical (OH), and nitrogen oxide radical (NO).[4] ROS attack most cellular components including lipids, carbohydrates, DNA, and proteins. When produced in excess ROS damage these components. Normally, the cells enzymatic systems and chemical scavengers remove the ROS formed in the cells. ROS therefore only becomes dangerous when the aforementioned systems are overwhelmed by production of excessive ROS. It has been suggested that multiple exposure of cells to ROS may alter gene expression to produce a cancerous tumor.[5] The level of molecular oxygen is directly proportional to the level of ROS in the cells. The probability for cellular damage or cell death increases with increasing levels of ROS and molecular oxygen.[6] It is therefore expected that exposure of cells to hypoxia would alter the intracellular oxygen balance and lead to an increase in intracellular oxygen tension. It should be noted that production of ROS does not always damage cells, since it is part of the cell's defense mechanism against pathogens. However, an excessive production of ROS is believed to be the cause of many diseases.[7]

The area of cellular analysis using fluorescence microscopy has grown in the last decade resulting in the development of a large number of cell permeable fluorescent probes.[8] Recent strides in the development of highly sensitive and relatively inexpensive charge couple device (CCD) cameras[9–11] have led to a dramatic improvement in the accuracy, reliability, and sensitivity of fluorescence microscopy measurements. The employment of laser scanning confocal microscopy has increased the spatial resolution of these measurements down to the diffraction limit ($\lambda/2$).[12] With these improvements, digital fluorescence imaging microscopy has become a

method of choice in cellular analysis. This paper describes a digital fluorescence imaging microscopy technique to monitor the response of murine macrophages to hypoxia, particularly the level of molecular oxygen in the cells. The number of analytical methods to measure oxygen levels in cells is surprisingly limited. Lau et al. used a Clark oxygen microelectrode to measure intracellular levels of molecular oxygen in neuron cells.[13] Clark electrodes have also been used to measure extracellular levels of molecular oxygen in cell culture media.[14] However, microelectrodes often fail in biological systems due to interfering electroactive species. Furthermore, the technique is not suitable in applications where a large number of cells need to be analyzed in real time. In our study, the oxygen sensitive luminescent indicator tris (1,10 phenanthroline) ruthenium (II) chloride $[Ru(phen)_3]$ is used for the first time, to measure in real time the level of molecular oxygen in cells. The luminescence properties of $Ru(phen)_3$ have been studied extensively by Demas et al.[15–18] The dye displays strong emission via metal-to-ligand charge transfer with a decay time of about 1 μs. It exhibits high molar absorption coefficient of $1.80 \times 10^4 \, M^{-1} cm^{-1}$ at 450 nm and high emission quantum emission yield (~ 0.5) at 604 nm,[19] which presents a large Stokes shift. Additionally, $Ru(phen)_3$ shows high photostability, high chemical stability, and water solubility, all of which lend to the usefulness of this dye in fluorescence quenching-based oxygen level measurements. $Ru(phen)_3$ has been used extensively as a luminescent oxygen indicator in fiber optic oxygen sensors and oxygen sensing films.[20–24] These sensors have been applied in aqueous samples[25,26] and biological fluids[27,28] but not for cellular imaging of oxygen. The employment of high performance digital fluorescence imaging technique enables the study of the response of a large number of cells simultaneously to hypoxia on a cell-by-cell basis. The hypoxia conditions are applied by suspending a cell sample in a glucose/glucose oxidase solution. Glucose oxidase catalyzes the oxidation of glucose. The reaction consumes oxygen, thus inducing conditions of external hypoxia.

2 Experimental

2.1 Digital Fluorescence Imaging Microscopy

The detection system used to measure the fluorescence of the oxygen sensitive dye, $Ru(phen)_3$, loaded into the cells is shown in Figure 1. The system consists of an inverted fluorescence microscopy (Olympus IX70) equipped with a 100 W mercury lamp as a light source. The fluorescence image of the cells is collected by a 20× microscope objective with a numerical aperture of 0.5. A 450 nm narrow-band excitation filter, a 500 nm dichroic mirror, and a 590 nm long-pass emission filter are used to ensure spectral imaging purity. The fluorescence signal is dispersed by a 150 mm three-mirror spectrograph (Acton Research Inc., Acton, MA) equipped with a 600 groves/mm grating blazed at an optimum wavelength of 500 nm. The grating can be replaced with a mirror, and the exit slit can be removed from the path of the fluorescence signal to allow the image of the cells to pass through the spectrograph without being dispersed by the grating. A high-performance CCD camera (Roper Scientific, Princeton, NJ, model 256HB) with a 512×512 pixel array is used for spectroscopic imaging or for digital fluorescence imaging of the cells. An exposure time 0.5 s is used for image collection.
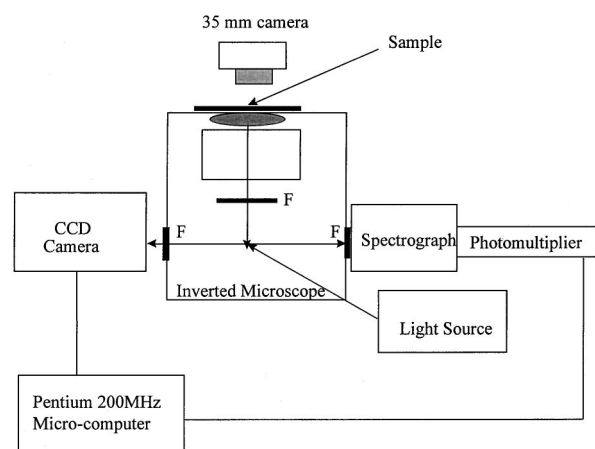

Fig. 1 Digital fluorescence imaging microscopy system. The experimental setup consists of an inverted fluorescence microscope with a 20× objective (NA=0.5), a high-performance CCD camera (Roper Scientific, 16-bit resolution, 512×512 chip size), and a microcomputer for image analysis.

A PC microcomputer (Gateway 2000, Pentium 200 MHz) is employed for data acquisition and the Rupert Scientific software WinSpec/32 is used for image analysis.

2.2 Fluorescence Spectroscopy Measurements

Excitation and emission spectra, as well as kinetic measurements are carried out using a PTI model QM-1 fluorometer (PTI, London, Ontario, Canada) equipped with a 75 W continuous Xe arc lamp as a light source.

2.3 Cell Culture

Cultures of J774 Murine Macrophages are maintained according to a standard protocol.[29] The cells are cultured in Dulbecco's modified Eagle's medium supplemented with 4 mM L-glutamine, 10 mM sodium bicarbonate, 25 mM glucose, 1 mM sodium pyruvate, and 10% fetal bovine serum. The cells are grown at 37 °C in 5% CO_2. The medium is replaced three times a week. To prepare subcultures, the cells are scraped in a new medium and split into new plates.

2.4 Loading of Cells with Ru(phen)₃

The macrophages are detached from the culture plate surface by scraping with a rubber policeman. The medium containing cells is centrifuged at 500 g for 10 min to precipitate the cells. Cells are collected and diluted to a concentration of about 10^6 cells/mL using a fresh medium. The concentration of the cells is determined by standard hemacytometry using Trypan Blue to assess cell viability. For the loading of the dye, 1 mL of cells $[(1-3) \times 10^6$ cells/mL], is incubated in the dark at 37 °C for 15 min with the appropriate volume of $Ru(phen)_3$ solution such that the dye concentration is 10^{-4} M in the solution. The cells are then washed three times with PBS buffer (pH 7.2) to remove excess free dye from the solution and from the surface of the cells.

2.5 Generation of Hypoxia Conditions using the Glucose/Glucose Oxidase System

An aliquot of glucose oxidase of 10 units/mL is added to 100 μL of a PBS buffer (pH 7.2) that contains 20 mM glucose and 10^6 cell/mL Ru(phen)$_3$ loaded cells. A 20 μL sample of this solution is placed between two microscope cover slips for fluorescence imaging. The sample is excited at 450 nm and the cells are imaged through a 20$\times$ objective. The first image is taken approximately 3 min after the reaction starts when movement of the cells stops. Subsequent images are taken every 4 min. An exposure time of 0.5 s is used for fluorescence image collection.

2.6 Materials and Reagents

Glucose and glucose oxidase (from Aspergillus niger) with enzymatic activity of 10 000 units/mL were purchased from Sigma. Tris (1,10-phenanthroline) ruthenium chloride (Ru(phen)$_3$) was purchased from Aldrich Chemical Company. Corning glass cover slips used for microscopy and pH buffers were purchased from Fisher Scientific. Aqueous solutions were prepared with 18 MΩ de-ionized water purification system (Barnstead Thermolyne Nanopure). J774 Murine Macrophages were purchased from ATCC (American Type Culture Collection). The Dulbecco's modified Eagle's medium and bovine serum albumin were purchased from Sigma. All reagents were used as received, without further purification.

3 Results and Discussion

3.1 Spectroscopic Properties of Ru(phen)$_3$

As previously mentioned ruthenium diimine complexes have been widely used as oxygen indicators in gas and aqueous samples. In this study the fluorescence properties of Ru(phen)$_3$ are used to monitor changes in J774 Macrophages as a result of external hypoxia. Ru(phen)$_3$ shows a strong absorption in the visible region ($\lambda_{max} = 450$ nm, $\epsilon = 18\,100$ M^{-1} cm^{-1}), a high-emission quantum yield of $\sim$0.5 at 604 nm, and a long excited-state lifetime ($\sim$1 μs). A concentration dependence of the fluorescence intensity of Ru(phen)$_3$ at 600 nm ($\lambda_{ex} = 450$ nm) in aqueous solution using a fluorometer, is shown in Figure 2. The fluorescence intensity of the free dye increases with increasing dye concentrations. However, at concentrations higher than 1×10^{-4} M, the fluorescence intensity decreases with increasing concentrations, a phenomenon that is attributed to self-quenching of the fluorescence signal.[26]

3.2 Oxygen Sensitivity of Ru(phen)$_3$

The fluorescence spectra of Ru(phen)$_3$ in nitrogen, air, and oxygen saturated solutions are shown in Figure 3. The fluorescence measurements are performed using a spectrofluorometer. Due to dynamic quenching by molecular oxygen, the fluorescence intensity of Ru(phen)$_3$ in nitrogen saturated solution $I(N_2)$ is higher than that in air saturated solution $I(\text{air})$, which is also higher than the fluorescence intensity of the oxygen saturated solution $I(O_2)$. The response factor $I(N_2)/I(O_2) = 7$. The analytical range of an oxygen probe is governed by the respective quenching curve and the Stern–

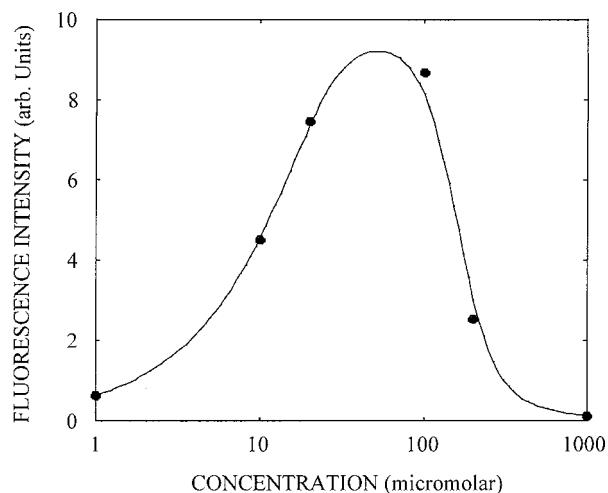**Fig. 2** Fluorescence intensity of Ru(phen)$_3$ in solution as a function of its concentration. A 450 nm light is used for excitation. Self-quenching occurs at concentrations greater than 1×10^{-4} M.

Volmer constant. The variation in the fluorescence intensity as a function of the dissolved oxygen concentration is given by the Stern–Volmer equation:

$$I_0/I_c = 1 + K_{SV}[O_2],$$

where I_0 is the fluorescence intensity of Ru(phen)$_3$ in a nitrogen-saturated solution, I_c is the fluorescence intensity of Ru(phen)$_3$ in a given dissolved oxygen concentration and K_{SV} is the Stern–Volmer quenching constant. In principle, higher quenching constants result in higher accuracy at low levels of oxygen. This is due to the larger signal change per oxygen concentration interval. However, high quenching constants re-
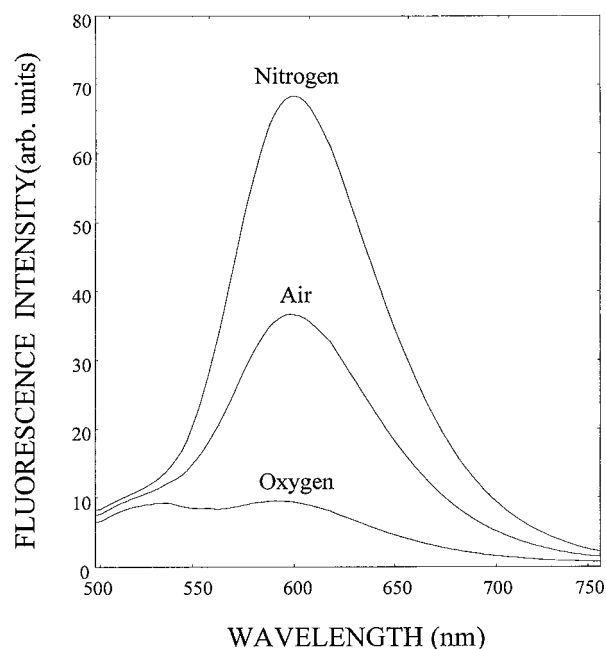

Fig. 3 Spectral response of Ru(phen)$_3$ of nitrogen, air, and oxygen saturated solutions when excited at 450 nm. Emission maximum is obtained at 604 nm.
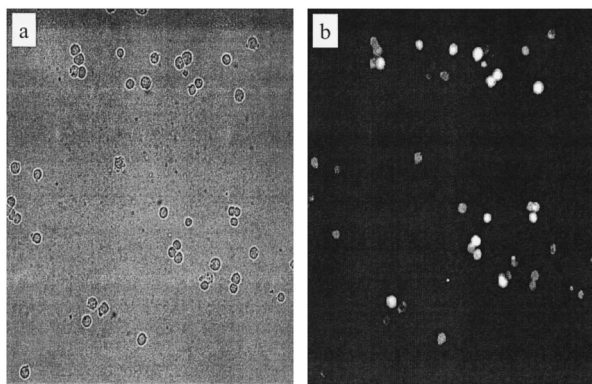
Fig. 4 Digital transmission (a) and fluorescence (b) images of Ru(phen)$_3$ loaded cells. A 10 μL sample is placed between two microscope slips, and fluorescence is detected and imaged by a CCD camera. A fluorescence filter cube consisting of a 450±10 nm excitation filter, a 500 nm dichroic mirror, and a 515 nm long band emission filter is used for imaging.

Fig. 5 Digital fluorescence images of Ru(phen)$_3$ loaded cells taken (a) 5 min and (b) 30 min, respectively, after enzymatic reaction begins. A 10 μL sample is placed between two microscope slips, and fluorescence is detected and imaged by a CCD camera. A fluorescence filter cube consisting of a 450±10 nm excitation filter, a 500 nm dichroic mirror, and a 515 nm long band emission filter is used for imaging.

sult in a more limited linear dynamic range. In a previous paper we described oxygen concentration dependent fluorescence measurements of Ru(phen)$_3$ in aqueous media.[26] We found that K_{SV} for Ru(phen)$_3$ is about 5420 M^{-1}. We also found a linear dynamic range between 0.1 and 12 ppm of molecular oxygen with a correlation coefficient of 0.996. We found a standard deviation of around 4% between ten consecutive fluorescence measurements in air saturated solutions. The standard deviation increases at lower oxygen levels when two large fluorescence intensities are subtracted from each other to obtain a small intensity difference. The accuracy of the oxygen measurement is governed by the uncertainties in the determination of I_0 (nitrogen saturated solution), K_{SV}, and I_c. An accurate determination of I_0 is essential for obtaining sufficiently accurate calibration curve and K_{SV} value.

3.3 Stability of Loaded Cells with Respect to Leaking and Photobleaching

Under our experimental conditions a 10^{-4} M Ru(phen)$_3$ solution is used for loading Ru(phen)$_3$ into the cells. Since the dye passively diffuses into the cells, the efficiency of permeation is nearly 100%. Transmission and fluorescence images of cells loaded with Ru(phen)$_3$ are shown in Figure 4. Figure 4(a) shows a transmission image of the cells taken with an exposure time of 3 ms. Figure 4(b) shows the fluorescence image of the same cells taken with an exposure time of 0.5 s. The images are taken using a 20× microscope objective [numerical aperture (NA)=0.5]. Monitoring the fluorescence intensity of the cells for 1 h shows a minimal leakage of Ru(phen)$_3$ from the cells.

The photobleaching rate of Ru(phen)$_3$ has previously been studied in our laboratory.[22] To monitor the rate of photobleaching of Ru(phen)$_3$ loaded cells under our experimental conditions, a 10 μL sample of the solution is placed between two microscope cover slips. The sample is then placed on the microscope stage and illuminated continuously at 450 nm. The fluorescence intensity of the cells decreases by approximately 5% during 30 min of continuous illumination. During our kinetic measurements the cells are exposed to the excita-
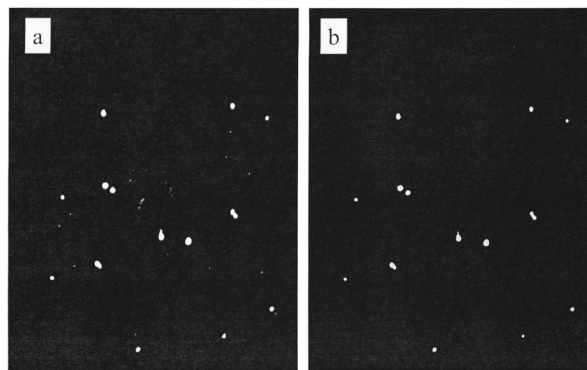
tion light for less than 1 s in each measurement. Each experiment lasts 30 min and images are taken in 3–5 min intervals. We therefore conclude that under our experimental conditions the loaded cells remain photostable throughout the experiment.

3.4 Response of Single Cells to Hypoxia

Since our samples are volume limited ($\sim$10 μL) it is practically impossible to physically change the extracellular concentrations of oxygen in the observed samples. The response of individual cells to conditions of hypoxia is therefore demonstrated by monitoring the enzymatic oxidation of glucose when a glucose/glucose oxidase solution is added to a microscope cover slip covered with cells. Glucose oxidase catalyzes the oxidation of glucose as follows:

$$\text{glucose} + O_2 \rightarrow \text{gluconic acid} + H_2O_2.$$

Molecular oxygen is consumed during this enzymatic oxidation. Figure 5(a) shows the fluorescence image of loaded cells taken 5 min after the start of the enzymatic reaction. The signal to noise ratio between the fluorescent cells and the background signal is found to be 80. Figure 5(b) shows the fluorescence images of loaded cells taken at 30 min after the start of the enzymatic reaction. The signal to noise ratio is 50. The cells maintain their structural integrity. There is about 30% variation in the fluorescence intensity of the Ru(phen)$_3$ loaded cells. This variation is due to the heterogeneity of the cellular sample, which contains viable cells at different growth stages and even dead cells. Viability measurements using a standard Trypan Blue method shows that the percentage of viable cells in a typical cellular sample is around 70%. Nevertheless, the variation in the relative decrease in signal of individual loaded cells as the enzymatic reaction progress is only 10%. The dye molecules distribute evenly in the cells and there is no evidence of compartmentalization. In Figure 6 the fluorescence intensity of single loaded cells is plotted against the enzymatic reaction time coordinate at different levels of glucose oxidase activity and cell viability. Each curve represents the average response of ten cells. Curve (a) describes the results of a control experiment in which the cells
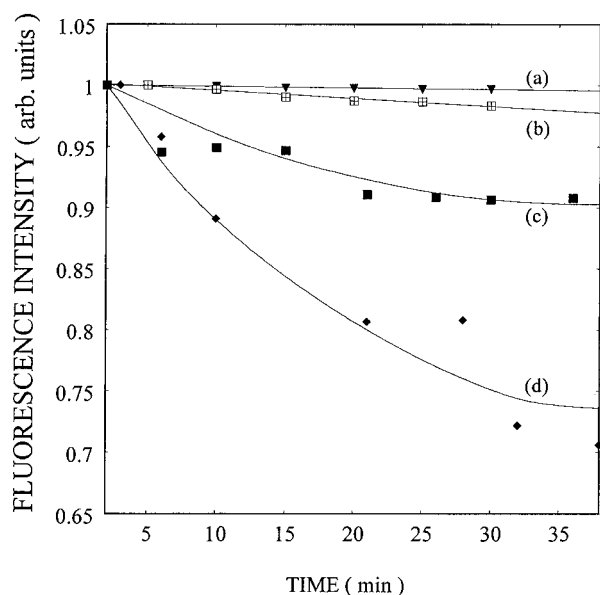
Fig. 6 The response of macrophages to hypoxia. Curve (a) describes the fluorescence intensity of the cells in the absence of glucose oxidase (normal conditions). Curve (b) describes the fluorescence intensity of dead cells in the presence of glucose and glucose oxidase. Curves (c) and (d) show a decrease in the fluorescence intensity of the cells when incubated with a solution containing 10 mM glucose and 10 units/mL (c) and 20 units/mL (d) glucose oxidase.

are suspended in a solution of 10 mM glucose in the absence of glucose oxidase. Curve (b) describes a control experiment in which the Ru(phen)$_3$ loaded cells were left for 24 h in a PBS buffer solution under ambient conditions. Unlike under normal storage conditions in a cell culture medium, 5% CO_2 atmosphere and 37 °C, the cells stop growing and die. Trypan Blue measurements show that under these conditions only about 10% of the cells remain viable after 24 h. These cells were suspended in a solution containing 10 mM glucose and 10 units/mL glucose oxidase. Both curves (a) and (b) show no noticeable change in the signal level due to hypoxia. Curves (c) and (d) describe the fluorescence intensity of viable cells when suspended in solutions containing 10 mM glucose and 10 units/mL (c) and 20 units/mL (d) of glucose oxidase. A 30% decrease in the fluorescence intensity of the cells is observed, indicating an interaction of Ru(phen)$_3$ with reactive oxygen species or production of molecular oxygen in the cells. Once the glucose/glucose oxidase solution is removed and replaced with glucose oxidase free buffer solution, the fluorescence intensity of the cells recovers to about 90% of its original value in about 20 min.

4 Summary and Conclusions

A high-resolution digital fluorescence imaging microscopy is used for the first time to follow the response of the oxygen sensitive fluorescent dye Ru(phen)$_3$ loaded into Murine Macrophages to hypoxia in real time. Ru(phen)$_3$ shows high photostability in cells, minimal dye leakage, a high emission quantum yield, and a large Stokes shift, which eliminates interference by cellular autoflourescence. Because of the high photostability of the dye, we have been able to quantitatively measure the fluorescence of the same living cells during ex-

periments that last 30 min without noticeable photobleaching. Control experiments in which the loaded cells were continuously exposed to the excitation light for 30 min show that the fluorescence intensity of the dye remains constant in living cells. The fluorescence of the loaded cells decreases by 30% when exposed to external hypoxia. The fluorescence decrease is attributed to the cellular production of molecular oxygen when the cells are exposed to hypoxia. The fluorescence intensity recovers to about 90% of its original fluorescence intensity once normal conditions are restored. This study offers a simple and direct way to monitor changes in oxygen levels in cells when they are exposed to external hypoxia. It is however possible that other processes contribute to the decrease in the fluorescence intensity of the dye when the cells are exposed to hypoxia. For example, it is possible that other quenching species are expressed when the cells are exposed to hypoxia. It is also possible that the increasing levels of reactive oxygen species leads to oxidation of Ru(phen)$_3$, which results in a decrease in the fluorescence intensity. The reversibility of the process suggests that any oxidized form of Ru(phen)$_3$ is unstable and readily reduced back to Ru(phen)$_3$ once normal oxygen conditions are restored.

References

1. B. W. McIlroy, A. Curnow, G. Buonaccorsi, M. A. Scott, S. G. Brown, and A. MacRobert, ''Spatial measurement of oxygen levels during photodynamic therapy using time-resolved optical spectroscopy,'' *J. Photochem. Photobiol., B* **43**, 47–55 (1998).
2. J. Kelley, ''Cytokines of the lung,'' *Am. Rev. Respir. Dis.* **141**, 765–788 (1990).
3. K. Kienast, M. Knorst, S. Lubjuhn, M. Muller-Quernheim, and R. Ferlinz, ''Nitrogen dioxide-induced reactive oxygen intermediates production by human alveolar macrophages and peripheral blood mononuclear cells,'' *Arch. Environ. Health* **49**, 246–250 (1994).
4. G. Tortora, B. Funke, and C. L. Case, *Microbiology*, 5th ed., p. 413, Benjamin/Cummings (1995).
5. *Free Radicals in Molecular Biology, Aging and Disease*, R. S. Armstrong, R. G. Sohal, R. G. Cutler, and T. F. Slater, Eds., Raven, New York (1984).
6. M. Martinez-Cayuela, ''Oxygen free radicals and human disease,'' *Biochimie* **77**, 147–161 (1995).
7. V. M. Reddy, ''Mechanism of mycobacterium avium complex pathogenesis,'' *Front Biosci.* **3**, 525–531 (1998).
8. R. P. Haugland, *Handbook of Fluorescent Probes and Research Chemicals*, 6th ed., Chap. 15, pp. 16, 21, Molecular Probes Inc., Eugene.
9. J. V. Sweedler, R. B. Bilhorn, G. R. S. Epperson, and M. B. Denton, ''High performance charge transfer device detectors,'' *Anal. Chem.* **60**, 282A–291A (1988).
10. J. V. Sweedler, R. B. Bilhorn, G. R. S. Epperson, and M. B. Denton, ''Applications of charge transfer devices in spectroscopy,'' *Anal. Chem.* **60**, 327A–335A (1988).
11. Q. S. Hanley, C. W. Earle, F. M. Pennebaker, S. P. Madden, and M. B. Denton, ''Charge transfer devices in analytical instrumentation,'' *Anal. Chem.* **68**, 661A–667A (1996).
12. G. N. Georgiou, M. T. Ahmet, A. Houlton, J. Silver, and J. Cherry, ''Measurement of the rate of uptake and subcellular localization of porphyrins in cells using fluorescence digital imaging microscopy,'' *Photochem. Photobiol.* **59**(4), 419 (1994).
13. Y. Y. Lau, T. Abe, and A. G. Ewing, ''Voltammetric measurement of oxygen in single neurons using platinized carbon ring electrodes,'' *Anal. Chem.* **64**(15), 1702–1705 (1992).

14. P. Connoly, P. Clark, A. S. Curtis, J. A. Dow, and C. D. Wilkinson, ''An extracellular microelectrode array for monitoring electrogenic cells in culture,'' *Biosens. Bioelectron.* **5**(3), 223–234 (1990).
15. E. R. Carraway, J. N. Demas, B. A. DeGraff, and J. R. Bacon, ''Photophysics and photochemistry of oxygen sensors based on luminescent transition-metal complexes,'' *Anal. Chem.* **63**, 337–342 (1991).
16. J. N. Demas and B. A. DeGraff, ''Design and applications of highly luminescent transition metal complexes,'' *Anal. Chem.* **63**, 829A–837A (1991).
17. L. Sacksteder, J. N. Demas, and B. A. DeGraff, ''Design of oxygen sensors based on quenching of luminescent metal complexes: Effect of ligand size on heterogeneity,'' *Anal. Chem.* **65**, 3480–3483 (1993).
18. W. Xu, R. C. McDonough III, B. Langsdorf, J. N. Demas, and B. A. DeGraff, ''Oxygen sensors based on luminescence quenching: interactions of metal complexes with the polymer supports,'' *Anal. Chem.* **66**, 4133–4141 (1993).
19. P. Hartmann, ''Photochemically induced energy-transfer effects on the decay times of ruthenium complexes in polymers,'' **72**, 2828–2834 (2000).
20. *Fiber Optic Chemical Sensors and Biosensors*, O. S. Wolfbeis, Ed., Chemical Rubber Corp., Boca Raton (1991).
21. Z. Rosenzweig and R. Kopelman, ''Development of a submicrometer optical fiber oxygen sensor,'' *Anal. Chem.* **67**, 2650–2654 (1995).
22. K. P. McNamara and Z. Rosenzweig, ''Dye-encapsulating liposomes as fluorescence-based oxygen nanosensors,'' *Anal. Chem.* **70**, 4853–4859 (1998).
23. K. P. McNamara and Z. Rosenzweig, ''Liposome-based optochemical nanosensors,'' *Mikrochim. Acta* **131**, 57–64 (1999).
24. H. A. Clark, M. Hoyer, M. A. Philbert, and R. Kopelman, ''Optical nanosensors for chemical analysis inside single living cells. 1. Fabrication, characterization, and methods for intracellular delivery of PEBBLE sensors,'' *Anal. Chem.* **71**, 4831–4836 (1999).
25. Z. Rosenzweig and R. Kopelman, ''Analytical properties and sensor size effects of a micrometer-sized optical fiber glucose biosensor,'' *Anal. Chem.* **68**, 1408–1413 (1996).
26. Z. Rosenzweig and R. Kopelman, ''Analytical properties of miniaturized oxygen and glucose fiber optic sensors,'' *Sens. Actuators B* **35–36**, 475–483 (1996).
27. D. B. Papkovsky, T. C. O'Riordan, and G. G. Guilbault, ''An immunosensor based on the glucose oxidase label and optical oxygen detection,'' *Anal. Chem.* **71**, 1568–1573 (1999).
28. R. Ruffolo, C. E. B. Evans, X. Liu, Y. Ni, Z. Pang, P. Park, A. R. McWilliams, X. Gu, A. Yekta, M. A. Winnik, and I. Manners, ''Phosphorescent oxygen sensors utilizing sulfur-nitrogen-phosphorus polymer matrixes: Synthesis, characterization, and evaluation of poly(thionylphosphazene)-b-poly(tetrahydrofuran) block copolymers,'' *Anal. Chem.* **72**, 1894–1904 (2000).
29. S. Gordon, ''The macrophage,'' *BioEssays* **17**(11), 977–986 (1995).